

Cocrystals of 5-fluorocytosine. I. Cofomers with fixed hydrogen-bonding sites

Maya Tutughamiarso,^a Guido Wagner^b and Ernst Egert^{a*}

^aInstitut für Organische Chemie und Chemische Biologie, Goethe-Universität Frankfurt, Max-von-Laue-Str. 7, 60438 Frankfurt am Main, Germany, and ^bInstitut für Anorganische und Analytische Chemie, Goethe-Universität Frankfurt, Max-von-Laue-Str. 7, 60438 Frankfurt am Main, Germany

Correspondence e-mail:
egert@chemie.uni-frankfurt.de

Received 24 April 2012

Accepted 5 June 2012

The antifungal drug 5-fluorocytosine (4-amino-5-fluoro-1,2-dihydropyrimidin-2-one) was cocrystallized with five complementary compounds in order to better understand its drug–receptor interaction. The first two compounds, 2-aminopyrimidine (2-amino-1,3-diazine) and *N*-acetylcreatinine (*N*-acetyl-2-amino-1-methyl-5*H*-imidazol-4-one), exhibit donor–acceptor sites for $R_2^2(8)$ heterodimer formation with 5-fluorocytosine. Such a heterodimer is observed in the cocrystal with 2-aminopyrimidine (I); in contrast, 5-fluorocytosine and *N*-acetylcreatinine [which forms homodimers in its crystal structure (II)] are connected only by a single hydrogen bond in (III). The other three compounds 6-aminouracil (6-amino-2,4-pyrimidinediol), 6-aminoisocytosine (2,6-diamino-3*H*-pyrimidin-4-one) and acyclovir [acycloguanosine or 2-amino-9-[(2-hydroxyethoxy)methyl]-1,9-dihydro-6*H*-purin-6-one] possess donor–donor–acceptor sites; therefore, they can interact with 5-fluorocytosine to form a heterodimer linked by three hydrogen bonds. In the cocrystals with 6-aminoisocytosine (*Va*)–(*Vd*), as well as in the cocrystal with the antiviral drug acyclovir (VII), the desired heterodimers are observed. However, they are not formed in the cocrystal with 6-aminouracil (IV), where the components are connected by two hydrogen bonds. In addition, a solvent-free structure of acyclovir (VI) was obtained. A comparison of the calculated energies released during dimer formation helped to rationalize the preference for hydrogen-bonding interactions in the various cocrystal structures.

1. Introduction

Pharmaceutical cocrystals contain at least one active pharmaceutical ingredient (API) and one cocrystal former, very often as a hydrogen-bonded molecular complex. They are attractive for the pharmaceutical industry because they offer an opportunity to provide alternative solid-state modifications and thus to optimize the physical properties of APIs. The first systematic study was reported by Zerkowski & Whitesides (1994) concerning complexes of barbituric acid and melamine derivatives. During the last decade design strategies, characterizations and applications of APIs have been investigated intensively (for overviews see Vishweshwar *et al.*, 2006; Yadav *et al.*, 2009).

One of the most promising strategies for designing a cocrystal is the usage of supramolecular synthons, which describe possible ways for complementary molecules to interact with each other by the formation of hydrogen bonds (Desiraju, 1995). Such synthons are well known from specific interactions between biologically important molecules. The most prominent example is the Watson–Crick base pairing, where complementary nucleobases (adenine/thymine and

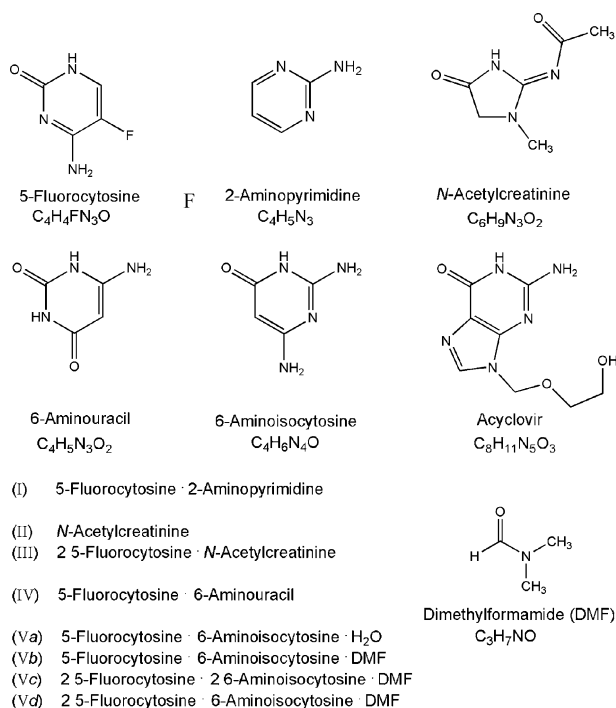
Table 1
Cocrystallization of 5-FC and 6-aminoisocytosine.

Crystal	5-FC (mg, mmol)	6-Aminoisocytosine (mg, mmol)	Solvent	Temperature (K)
(Va)	1.8, 0.014	1.8, 0.014	DMSO (60 μ L)	277
(Vb) and (Vc)	1.4, 0.011	2.1, 0.017	DMF (120 μ L)	323
(Vd)	1.8, 0.014	2.1, 0.017	DMF (80 μ L)	323

Table 2
Cocrystallization of 5-FC and acyclovir.

Crystal	5-FC (mg, mmol)	Acyclovir (mg, mmol)	Solvent	Temperature (K)
(VI)	1.3, 0.010	2.4, 0.011	DMAC (50 μ L)	323
(VII)	1.5, 0.012	2.6, 0.012	DMF (50 μ L)	323

guanine/cytosine) are hydrogen-bonded to each other. Furthermore, the complementary pattern in hydrogen-bond formation is very often essential for the recognition between a drug and its receptor.



Scheme 1

5-Fluorocytosine (5-FC) is one of the oldest antifungal drugs. It becomes active after conversion into its toxic metabolite 5-fluorouracil by the enzyme cytosine deaminase (CD; Morschhäuser, 2003). 5-Fluorouracil inhibits the biosynthesis of fungal DNA and RNA by two major mechanisms: inhibition of thymidylate synthase by 5-fluorodeoxyuridine monophosphate and incorporation of 5-fluorouridine triphosphate into fungal RNA (Vermes *et al.*, 2000). Since resistance develops during treatment, monotherapy with 5-FC is limited and only

applied in some cases of chromoblastomycosis and in uncomplicated lower urinary tract candidiasis as well as vaginal candidiasis (Benson & Nahata, 1988); in all other cases, it is administered together with amphotericin B (Francis & Walsh, 1992). In combination with the bacterial CD gene, however, 5-FC can be used as a suicide enzyme–prodrug system in gene therapy for the treatment of cancer (Huber *et al.*, 1994).

Due to our interest in studying its drug–receptor interaction, we cocrystallized 5-fluorocytosine with five compounds containing complementary functional groups (Scheme 1), with the aim of obtaining complexes held together by N–H...O and N–H...N hydrogen bonds.

2. Experimental

2.1. Sample preparation

Almost all reagents are commercially available and were used without further purification. Single crystals of (I) were obtained by cocrystallization of 5-FC (2.3 mg, 0.018 mmol) and 2-aminopyrimidine (1.7 mg, 0.018 mmol) in dimethylacetamide (250 μ L) at 323 K. *N*-Acetylcreatinine was prepared from creatinine (5 g, 0.044 mol) by reaction with acetic anhydride (10.4 ml, 0.110 mol) in 1,4-dioxane (100 ml). After refluxing at 383 K for 24 h, the mixture was cooled to room temperature and the solvent was removed producing a yellow powder (4.18 g, 61% yield). Crystals of (II) were obtained by recrystallization of *N*-acetylcreatinine (4.4 mg, 0.028 mmol) from methanol (300 μ L) at room temperature. Cocrystallization of 5-FC (2.3 mg, 0.018 mmol) and *N*-acetylcreatinine (2.5 mg, 0.016 mmol) from dimethyl sulfoxide (50 μ L) at room temperature yielded crystals of (III). Crystals of (IV) were obtained by solvent evaporation experiments with mixtures of 5-FC (1.8 mg, 0.014 mmol) and 6-aminouracil (3.9 mg, 0.031 mmol) in dimethyl sulfoxide (120 μ L) at 323 K. Cocrystallization of 5-FC and 6-aminoisocytosine yielded four pseudopolymorphs (Va)–(Vd) (Table 1), while crystals of (VI) and (VII) were obtained by cocrystallization attempts with 5-FC and acyclovir (Table 2). None of the solvents used in the experiments were water-free.

2.2. Crystal structure determination

The X-ray diffraction data were collected on a Stoe IPDS II two-circle diffractometer using monochromatic Mo $K\alpha$ radiation ($\lambda = 0.71073$ Å) at 173 K. Data reduction and cell refinement were carried out with *X-AREA* (Stoe & Cie, 2001). All structures were solved by direct methods (*SHELXS97*; Sheldrick, 2008) and refined by full-matrix least-squares techniques (*SHELXL97*; Sheldrick, 2008).

All H atoms, except those bonded to disordered solvent atoms, were initially located by difference Fourier synthesis. Subsequently, H atoms bonded to C atoms were refined using a riding model, with methyl C–H = 0.98 Å, secondary C–H = 0.99 Å and aromatic C–H = 0.95 Å, and with $U_{iso}(H) = 1.5 U_{eq}(C)$ for methyl H or $1.2 U_{eq}(C)$ for secondary and aromatic H atoms. In (II), (IV), (Va), (Vc) and (VII), H atoms bonded

to N atoms were refined isotropically. In the other structures the isotropic displacement parameters of these H atoms were smaller than the equivalent isotropic displacement parameter of the respective N atom [$U_{\text{iso}}(\text{H}) < U_{\text{eq}}(\text{N})$]; thus they were coupled to those of the N atoms with $U_{\text{iso}}(\text{H}) = 1.2 U_{\text{eq}}(\text{N})$. Additionally, some N–H distances were restrained to 0.88 (2) Å (Table 3). The solvent water H atoms were refined isotropically in (Va). In (VI) and (VII) the hydroxy H atoms were refined using a riding model with O–H = 0.84 Å and with $U_{\text{iso}}(\text{H}) = 1.2 U_{\text{eq}}(\text{O})$.

One methyl group in (II) shows rotational disorder with a site-occupation factor of 0.74 (2) for the major occupied orientation. In (Vc) the centroid of the dimethylformamide molecule lies on an inversion centre, so that all solvent atoms are disordered. In (Vd) all C atoms of one dimethylformamide molecule are disordered over two positions with a site-occupation factor of 0.77 (1) for the major occupied site. The following restraints were applied during refinement of the solvent molecules in (Vc) and (Vd): $\text{O}=\text{C}_{\text{carbonyl}} = 1.24$ (2), $\text{C}_{\text{carbonyl}}-\text{N} = 1.32$ (2), $\text{N}-\text{C}_{\text{methyl}} = 1.45$ (2), $\text{O}\cdots\text{N} = 2.27$ (4), $\text{C}_{\text{carbonyl}}\cdots\text{C}_{\text{methyl}} = 2.42$ (4) and $\text{C}_{\text{methyl}}\cdots\text{C}_{\text{methyl}} = 2.48$ (4) Å. The C and N atoms of the minor occupied site in (Vd) were refined isotropically.

For structural drawings the following programs were used: *Mercury* (Version 2.3; Macrae *et al.*, 2008) and *XP* (Sheldrick, 2008). Selected crystal data and experimental details are summarized in Table 4.¹

2.3. *Ab initio* calculations

Starting molecular geometries were generated either from crystal data or from molecular sketches using *Avogadro* (*Avogadro*: an open-source molecular builder and visualization tool, Version 1.0.3, <http://avogadro.openmolecules.net/>). *Ab initio* energy calculations were performed with geometry optimization and dispersion correction using *GAUSSIAN* (Frisch *et al.*, 2004) at the B3LYP-D/6-311++G** level. A counterpoise correction was applied to all dimers selected.

3. Results

5-FC exhibits two potential hydrogen-bonding sites: an acceptor–acceptor–donor (*AAD*; *A*: hydrogen-bond acceptor and *D*: hydrogen-bond donor) and an acceptor–donor (*AD*) site. In its polymorphs and pseudopolymorphs, it prefers the formation of $R_2^2(8)$ homodimers (Bernstein *et al.*, 1995) usually characterized by one N–H \cdots O and one N–H \cdots N hydrogen bond (Tutughamiarso *et al.*, 2009). Only in one monohydrate structure are the homodimers stabilized by either two N–H \cdots O or two N–H \cdots N hydrogen bonds [Cambridge Structural Database (CSD, Version 5.33 of November 2011, plus two updates; Allen, 2002) refcode BIRMEU03 (Hulme & Tocher, 2006)].

¹ Supplementary data for this paper are available from the IUCr electronic archives (Reference: GP5052). Services for accessing these data are described at the back of the journal.

Table 3

NH and NH₂ groups with restrained N–H distances.

Crystal	N atoms involved
(I)	N21, N41'
(III)	N1A, N41A, N1B, N41B
(Vb)	N3, N21, N61, N1', N41'
(Vc)	N61, N1'
(Vd)	N21A, N61A, N1B, N41B, N41C, N3D, N61D, N1E, N41E, N1F, N41F, N3G, N1H, N41H, N1I, N41I
(VI)	N1, N21
(VII)	N1, N41'

Considering the *AAD* and *AD* sites as well as the favourable synthons for 5-FC, suitable cofomers with fixed hydrogen-bonding sites were selected for the cocrystallization experiments (Scheme 1). 2-Aminopyrimidine and *N*-acetylcreatinine possess at least one donor–acceptor (*DA*) site suited for $R_2^2(8)$ heterodimer formation with 5-FC. Due to their donor–donor–acceptor (*DDA*) site 6-aminouracil, 6-aminoisocytosine and acyclovir can even be linked to 5-FC by three hydrogen bonds.

3.1. Cocrystals with 2-aminopyrimidine and *N*-acetylcreatinine

Owing to its adjacent amine and imine groups 2-aminopyrimidine can be connected to 5-FC either by one N–H \cdots O and one N–H \cdots N hydrogen bond or by two N–H \cdots N hydrogen bonds. A similar $R_2^2(8)$ heterodimer between 5-FC and *N*-acetylcreatinine can be formed as well; in this case the heterodimer may be held together either by one N–H \cdots O and one N–H \cdots N hydrogen bond or by two N–H \cdots O hydrogen bonds.

The asymmetric unit of the 5-FC–2-aminopyrimidine (1/1) cocrystal (I) is shown in Fig. 1: both molecules are coplanar to each other (r.m.s. deviation = 0.057 Å for all non-H atoms) and are connected to an $R_2^2(8)$ heterodimer by one N–H \cdots O and one N–H \cdots N hydrogen bond. In the crystal packing two centrosymmetrically related heterodimers are stabilized by four N–H \cdots O hydrogen bonds forming an $R_4^2(8)$ motif; in addition, the 5-FC molecules are linked to an $R_2^2(8)$ homodimer by two N–H \cdots N hydrogen bonds (Fig. 2, Table 5). Altogether the packing of (I) shows ribbons parallel to ($\bar{1}20$).

Recrystallization of *N*-acetylcreatinine yielded crystal (II). The five-membered imidazolidinone ring is planar (r.m.s. deviation = 0.009 Å for all non-H atoms) and the C41 methyl group is disordered over two orientations. A dihedral angle of 19.1 (1)° is enclosed between the planes through the non-H atoms of the ring and those of the acetamide group with the side-chain atom O54 directed to the same side as the N1–H group, which enables an intramolecular hydrogen bond (Fig. 1). In the crystal packing two *N*-acetylcreatinine molecules are linked by two N–H \cdots O hydrogen bonds to a dimer, which forms layers parallel to ($\bar{1}03$) (Fig. 3, Table 6).

Complex (III) crystallized with two 5-FC molecules and one *N*-acetylcreatinine molecule in the asymmetric unit (Fig. 1). The 5-FC molecules – as in their (pseudo)polymorphs (Tutughamiarso *et al.*, 2009) – are connected to an $R_2^2(8)$

Table 4

Experimental details.

Experiments were carried out at 173 K with Mo $K\alpha$ radiation using a Stoe IPDS II two-circle diffractometer. H atoms were treated by a mixture of independent and constrained refinement.

	(I)	(II)	(III)	(IV)	(Va)
Crystal data					
Chemical formula	$C_4H_4FN_3O \cdot C_4H_5N_3$	$C_6H_9N_3O_2$	$2(C_4H_4FN_3O) \cdot C_6H_9N_3O_2$	$C_4H_4FN_3O \cdot C_4H_5N_3O_2$	$C_4H_4FN_3O \cdot C_4H_6-N_4O \cdot H_2O$
M_r	224.21	155.16	413.37	256.21	273.25
Crystal system, space group	Triclinic, $P\bar{1}$	Monoclinic, $P2_1/n$	Triclinic, $P\bar{1}$	Monoclinic, $C2/c$	Triclinic, $P\bar{1}$
a, b, c (Å)	6.2414 (12), 7.2335 (17), 11.546 (2)	7.9835 (14), 10.0664 (12), 9.8380 (16)	7.6548 (12), 9.3233 (14), 12.848 (2)	15.5508 (15), 11.7839 (7), 11.4971 (12)	8.3280 (12), 9.3484 (14), 9.4779 (15)
α, β, γ (°)	105.371 (18), 101.944 (16), 91.700 (18)	90, 111.266 (13), 90	83.406 (12), 83.529 (12), 81.420 (12)	90, 101.660 (8), 90	61.797 (11), 64.500 (11), 67.138 (11)
V (Å ³)	489.76 (17)	736.8 (2)	896.4 (2)	2063.4 (3)	570.83 (15)
Z	2	4	2	8	2
μ (mm ⁻¹)	0.12	0.11	0.13	0.14	0.14
Crystal size (mm)	0.40 × 0.10 × 0.10	0.40 × 0.20 × 0.20	0.30 × 0.30 × 0.20	0.60 × 0.30 × 0.30	0.30 × 0.30 × 0.15
Data collection					
Absorption correction	–	–	–	–	–
No. of measured, independent and observed [$I > 2\sigma(I)$] reflections	4298, 1834, 1246	4148, 1378, 1081	7962, 3344, 2293	15 020, 1935, 1507	6264, 2124, 1615
R_{int}	0.138	0.075	0.122	0.159	0.093
($\sin \theta/\lambda$) _{max} (Å ⁻¹)	0.608	0.608	0.610	0.608	0.609
Refinement					
$R[F^2 > 2\sigma(F^2)]$, $wR(F^2)$, S	0.072, 0.210, 0.95	0.048, 0.118, 0.97	0.063, 0.165, 0.95	0.037, 0.096, 0.99	0.047, 0.122, 0.96
No. of reflections	1834	1378	3344	1935	2124
No. of parameters	161	107	286	192	212
No. of restraints	4	0	6	0	0
$\Delta\rho_{max}$, $\Delta\rho_{min}$ (e Å ⁻³)	0.32, -0.38	0.21, -0.28	0.33, -0.31	0.27, -0.21	0.29, -0.28
	(Vb)	(Vc)	(Vd)	(VI)	(VII)
Crystal data					
Chemical formula	$C_4H_4FN_3O \cdot C_4H_6-N_4O \cdot C_3H_7NO$	$2C_4H_4FN_3O \cdot 2C_4H_6-N_4O \cdot C_3H_7NO$	$2C_4H_4FN_3O \cdot C_4H_6-N_4O \cdot C_3H_7NO$	$C_8H_{11}N_5O_3$	$C_4H_4FN_3O \cdot C_8H_{11}N_5O_3$
M_r	328.33	583.56	457.43	225.22	354.32
Crystal system, space group	Triclinic, $P\bar{1}$	Triclinic, $P\bar{1}$	Triclinic, $P\bar{1}$	Monoclinic, $P2_1/c$	Monoclinic, $P2_1/c$
a, b, c (Å)	9.0866 (14), 9.3632 (15), 9.4019 (15)	7.1894 (12), 10.0991 (15), 10.9953 (19)	11.2283 (11), 15.1837 (12), 18.8290 (17)	10.9182 (11), 11.1666 (8), 7.9786 (9)	7.0859 (5), 9.0414 (5), 22.8754 (16)
α, β, γ (°)	104.720 (13), 94.340 (13), 102.010 (13)	104.97 (1), 105.33 (1), 110.85 (1)	71.262 (7), 87.187 (8), 88.460 (7)	90, 108.346 (8), 90	90, 98.155 (6), 90
V (Å ³)	749.7 (2)	662.22 (19)	3036.1 (5)	923.30 (15)	1450.73 (16)
Z	2	1	6	4	4
μ (mm ⁻¹)	0.12	0.12	0.13	0.13	0.13
Crystal size (mm)	0.60 × 0.60 × 0.30	0.50 × 0.50 × 0.40	0.30 × 0.20 × 0.15	0.20 × 0.10 × 0.10	0.60 × 0.60 × 0.40
Data collection					
Absorption correction	–	–	–	–	–
No. of measured, independent and observed [$I > 2\sigma(I)$] reflections	8452, 2806, 1593	7507, 2475, 1665	32 977, 10 672, 5218	6501, 1723, 1215	11 519, 2718, 2202
R_{int}	0.080	0.074	0.097	0.132	0.073
($\sin \theta/\lambda$) _{max} (Å ⁻¹)	0.608	0.608	0.595	0.607	0.610
Refinement					
$R[F^2 > 2\sigma(F^2)]$, $wR(F^2)$, S	0.048, 0.106, 0.89	0.057, 0.170, 1.07	0.060, 0.139, 0.90	0.058, 0.140, 0.99	0.039, 0.098, 0.95
No. of reflections	2806	2475	10 672	1723	2718
No. of parameters	235	242	981	155	252
No. of restraints	8	11	33	3	2
$\Delta\rho_{max}$, $\Delta\rho_{min}$ (e Å ⁻³)	0.29, -0.22	0.29, -0.23	0.62, -0.34	0.27, -0.31	0.34, -0.33

homodimer characterized by one N—H···O and one N—H···N hydrogen bond. The conformation of *N*-acetylcreatinine is similar to that in (II): the N1—H and C52—O54 groups are again oriented in the same direction, but the dihedral angle between the planes through the ring and the amide group is now 32.1 (2)° with an N1···O54 distance of 2.752 (3) Å. The planar imidazolidinone ring (r.m.s. deviation = 0.007 Å for all non-H atoms) and the 5-FC homodimer form

a dihedral angle of 42.0 (1)°, while the 5-FC molecules are twisted by 8.8 (1)° with respect to each other. In the crystal packing the 5-FC molecules form ribbons running along the *b* axis with repeated $R_2^2(8)$ dimer interactions. The *N*-acetylcreatinine molecules link the 5-FC ribbons to layers parallel to (101) by accepting two N—H···O hydrogen bonds (Fig. 4, Table 7). Further N—H···O interactions between *N*-acetylcreatinine and 5-FC bridge the layers to a three-dimensional

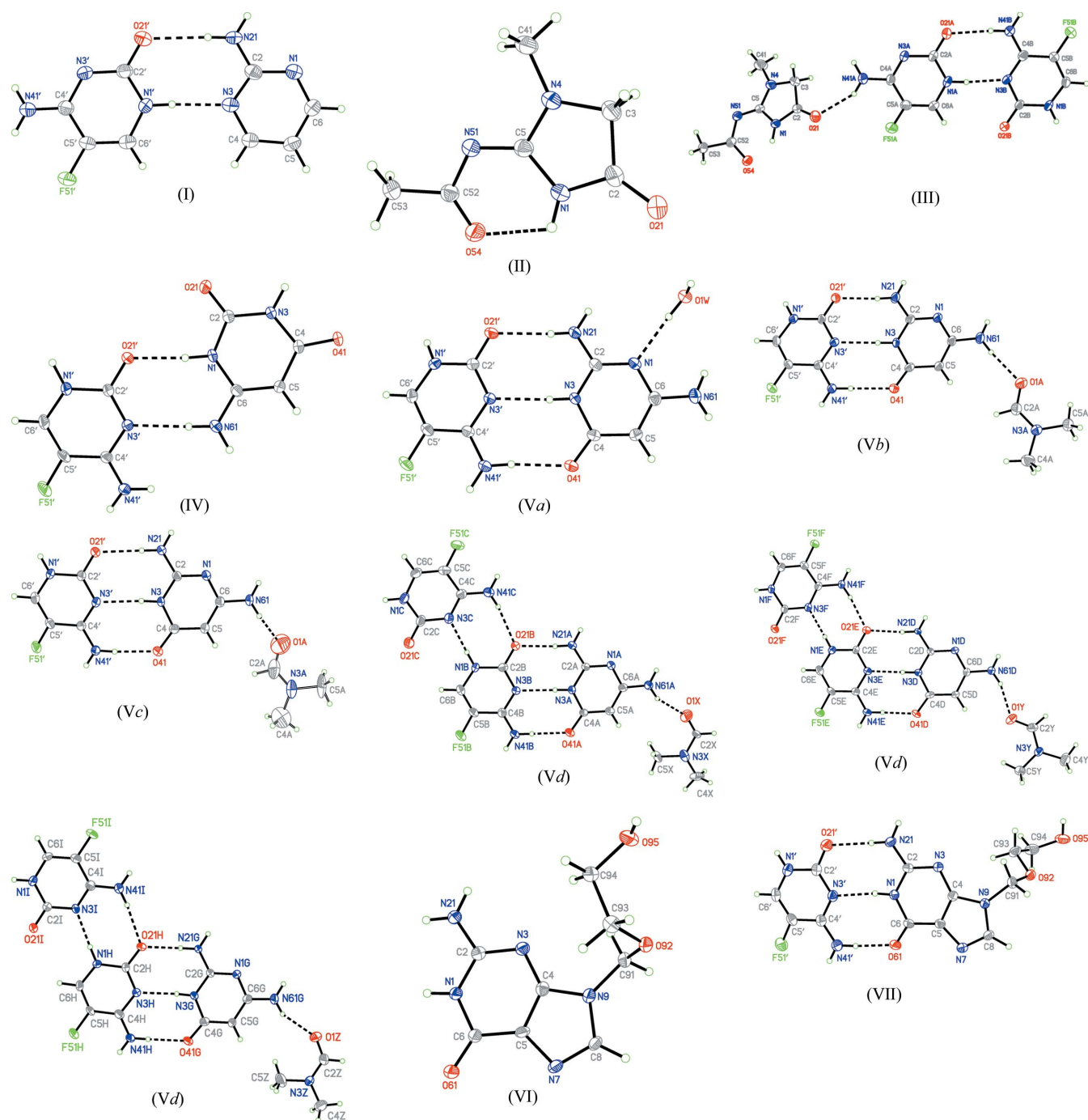


Figure 1

The asymmetric units and numbering schemes of (I)–(VII). Displacement ellipsoids are drawn at the 50% probability level and H atoms are shown as small spheres of arbitrary radii. Hydrogen bonds are shown as a dashed line. Only major occupied sites of the methyl group in (II) as well as of the DMF molecules in (Vc) and (Vd) are shown.

Table 5
Hydrogen-bond geometry (Å, °) for (I).

$D-H\cdots A$	$D-H$ (Å)	$H\cdots A$ (Å)	$D\cdots A$ (Å)	$D-H\cdots A$ (°)
$N21-H21B\cdots O21^{ii}$	0.879 (19)	2.11 (2)	2.917 (3)	152 (3)
$N21-H21A\cdots O21'$	0.894 (19)	2.20 (2)	3.072 (4)	165 (3)
$N1'-H1'\cdots N3$	0.88 (4)	1.96 (4)	2.836 (4)	171 (3)
$N41'-H41B\cdots N3^{iii}$	0.879 (19)	2.09 (2)	2.967 (4)	173 (3)
$N41'-H41A\cdots N1^{iii}$	0.899 (19)	2.25 (2)	3.136 (3)	168 (3)

Symmetry codes: (i) $-x+2, -y+1, -z+1$; (ii) $-x+2, -y+1, -z+2$; (iii) $x, y, z+1$.

hydrogen-bonded network (Fig. 5), which might explain the increased twist of the side chain compared with (II).

3.2. Cocrystals with 6-aminouracil and 6-aminoisocytosine

In addition to their *DDA* hydrogen-bonding site, which allows the formation of three hydrogen bonds with 5-FC, 6-aminouracil also possesses an acceptor–donor–acceptor (*ADA*) site, while 6-aminoisocytosine exhibits a donor–acceptor–donor (*DAD*) site. If the desired *AAD/DDA* heterodimer is formed, these additional binding sites can be $R_2^2(8)$ hydrogen-bonded either to themselves or to another 5-FC molecule.

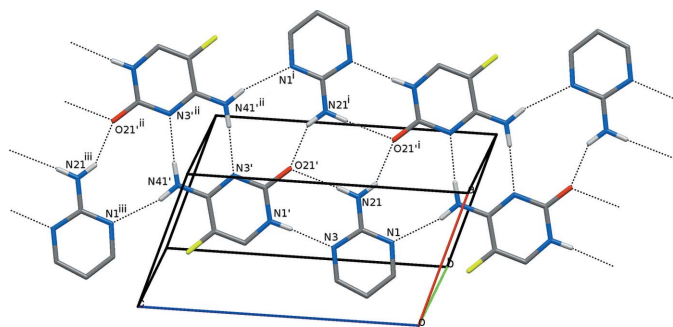


Figure 2
Partial packing diagram for (I). Dashed lines indicate hydrogen bonds. Only the H atoms involved in hydrogen bonding are shown. Symmetry codes: (i) $-x+2, -y+1, -z+1$; (ii) $-x+2, -y+1, -z+2$; (iii) $x, y, z+1$.

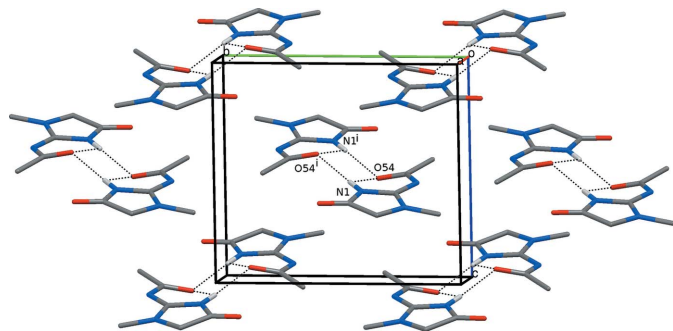


Figure 3
Partial packing diagram for (II), showing discrete arrangements of *N*-acetylcreatine dimers. Dashed lines indicate hydrogen bonds. Only the major occupied sites of the methyl groups and the H atoms involved in hydrogen bonding are shown. Symmetry code: (i) $-x, -y+1, -z+1$.

Table 6
Hydrogen-bond geometry (Å, °) for (II).

$D-H\cdots A$	$D-H$ (Å)	$H\cdots A$ (Å)	$D\cdots A$ (Å)	$D-H\cdots A$ (°)
$N1-H1\cdots O54^i$	0.86 (3)	2.02 (3)	2.849 (2)	162 (2)
$N1-H1\cdots O54$	0.86 (3)	2.29 (2)	2.720 (2)	111.0 (19)

Symmetry code: (i) $-x, -y+1, -z+1$.

The asymmetric unit of cocrystal (IV) contains one 5-FC and one 6-aminouracil molecule (Fig. 1). Although both compounds are essentially planar (r.m.s. deviations = 0.023 Å for all non-H atoms of 5-FC and 0.016 Å for those of 6-aminouracil), a dihedral angle of 19.7 (1)° is enclosed between the planes of the two molecules. The desired complex with three hydrogen bonds is not formed; instead both molecules are connected to another heterodimer by one $N-H\cdots O$ and one $N-H\cdots N$ hydrogen bond with an $R_2^2(8)$ pattern. Additionally each compound forms centrosymmetric $R_2^2(8)$ homodimers characterized by two $N-H\cdots O$ hydrogen bonds, thus forming chains of alternating hetero- and homodimers parallel to (201) (Fig. 6a, Table 8). Along the *b* axis further chains consisting of alternating homodimers of 5-FC and 6-aminouracil are stabilized by three $N-H\cdots O$ interactions with an $R_3^2(8)$ hydrogen-bonding pattern (Fig. 6b). Altogether

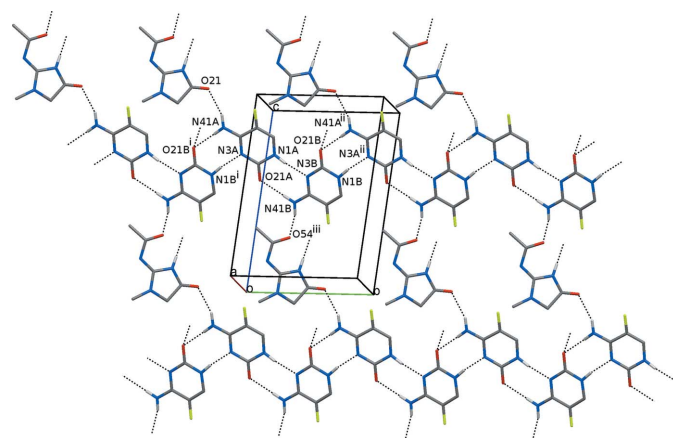


Figure 4
Partial packing diagram for (III). Dashed lines indicate hydrogen bonds. Only the H atoms involved in hydrogen bonding are shown. Symmetry codes: (i) $x, y-1, z$; (ii) $x, y+1, z$; (iii) $x-1, y+1, z-1$.

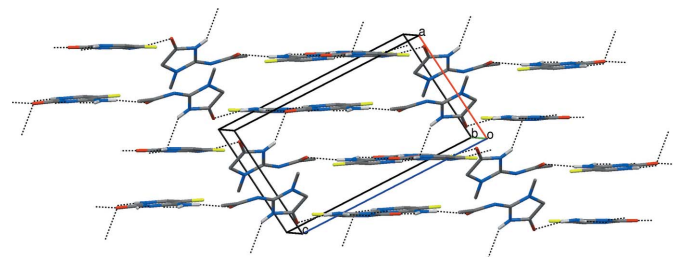


Figure 5
Partial packing diagram for (III), showing the three-dimensional hydrogen-bonded network. Dashed lines indicate hydrogen bonds. Only the H atoms involved in hydrogen bonding are shown.

the packing shows an extended three-dimensional hydrogen-bonded network (Fig. 7).

Four cocrystals, (Va)–(Vd), were obtained during the cocrystallization attempts of 5-FC with 6-aminoisocytosine. In contrast to (IV) the desired *AAD/DDA* heterodimers with N–H···O and N–H···N hydrogen bonds similar to the Watson–Crick C–G base pair are always formed. An $R_4^2(8)$ hydrogen-bonding pattern consisting of four N–H···O interactions is also observed in the four cocrystal structures; it links two heterodimers to a tetramer.

In (Va) the complex between 5-FC and 6-aminoisocytosine crystallized as a monohydrate (Fig. 1). The planes through the non-H atoms of 5-FC and those of 6-aminoisocytosine enclose a dihedral angle of $7.1(1)^\circ$. In the crystal packing the heterodimers are connected to ribbons by two different $R_4^2(8)$ patterns (each with four N–H···O hydrogen bonds; Fig. 8, Table 9). The ribbons run parallel to $(\bar{1}12)$ and are stabilized to

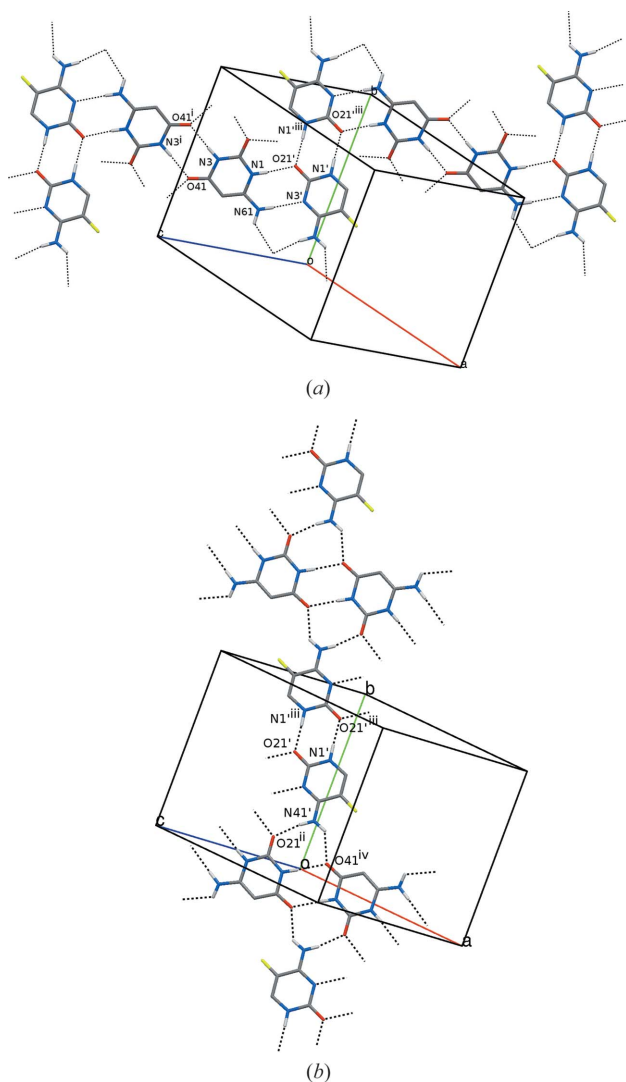


Figure 6

Partial packing diagrams for (IV), showing chains running parallel to (201) (a) and along the *b* axis (b). Dashed lines indicate hydrogen bonds. Only the H atoms involved in hydrogen bonding are shown. Symmetry codes: (i) $-x, -y + 1, -z + 2$; (ii) $-x + \frac{1}{2}, y - \frac{1}{2}, -z + \frac{3}{2}$; (iii) $-x + \frac{1}{2}, -y + \frac{3}{2}, -z + 1$; (iv) $x + \frac{1}{2}, -y + \frac{1}{2}, z - \frac{1}{2}$.

Table 7

Hydrogen-bond geometry (\AA , $^\circ$) for (III).

<i>D</i> –H··· <i>A</i>	<i>D</i> –H (\AA)	H··· <i>A</i> (\AA)	<i>D</i> ··· <i>A</i> (\AA)	<i>D</i> –H··· <i>A</i> ($^\circ$)
N1A–H1A···N3B	0.898 (18)	1.883 (19)	2.778 (3)	175 (3)
N41A–H412···O21B ⁱ	0.886 (18)	2.066 (19)	2.950 (3)	175 (3)
N41A–H411···O21	0.891 (18)	2.13 (2)	2.946 (3)	153 (3)
N1B–H1B···N3A ⁱⁱ	0.898 (18)	1.911 (19)	2.802 (3)	171 (3)
N41B–H414···O21A	0.885 (18)	2.02 (2)	2.901 (3)	171 (3)
N41B–H413···O54 ⁱⁱⁱ	0.870 (18)	2.02 (2)	2.862 (3)	162 (3)
N1–H1···O21B ^{iv}	0.86 (3)	2.06 (3)	2.817 (3)	147 (3)

Symmetry codes: (i) $x, y - 1, z$; (ii) $x, y + 1, z$; (iii) $x - 1, y + 1, z - 1$; (iv) $-x + 2, -y, -z + 2$.

Table 8

Hydrogen-bond geometry (\AA , $^\circ$) for (IV).

<i>D</i> –H··· <i>A</i>	<i>D</i> –H (\AA)	H··· <i>A</i> (\AA)	<i>D</i> ··· <i>A</i> (\AA)	<i>D</i> –H··· <i>A</i> ($^\circ$)
N1–H1···O21 ⁱ	0.90 (2)	1.88 (2)	2.7805 (17)	175.4 (17)
N3–H3···O41 ⁱ	0.93 (2)	1.92 (2)	2.8534 (17)	176.9 (19)
N61–H61A···O21 ⁱⁱ	0.90 (2)	2.62 (2)	3.1691 (18)	120.6 (18)
N61–H61B···N3 ⁱ	0.92 (3)	2.09 (3)	3.011 (2)	175.2 (19)
N1 ⁱ –H1 ⁱ ···O21 ⁱⁱⁱ	0.98 (2)	1.85 (2)	2.8256 (17)	173.3 (18)
N41 ⁱ –H41C···O41 ^{iv}	0.90 (2)	2.19 (2)	2.9012 (17)	135.7 (18)
N41 ⁱ –H41D···O21 ⁱⁱ	0.91 (2)	1.91 (2)	2.809 (2)	169.7 (19)

Symmetry codes: (i) $-x, -y + 1, -z + 2$; (ii) $-x + \frac{1}{2}, y - \frac{1}{2}, -z + \frac{3}{2}$; (iii) $-x + \frac{1}{2}, -y + \frac{3}{2}, -z + 1$; (iv) $x + \frac{1}{2}, -y + \frac{1}{2}, z - \frac{1}{2}$.

a three-dimensional network by further N–H···O interactions and by the water molecules, each of which is involved in three hydrogen bonds.

Crystallization attempts from dimethylformamide (DMF) yielded three cocrystal solvates, *viz.* (Vb), (Vc) and (Vd), whereby (Vb) and (Vc) were obtained from the same sample tube. The asymmetric unit of (Vb) consists of one hydrogen-bonded heterodimer and one DMF molecule; the three molecules are essentially coplanar to each other (r.m.s. deviation = 0.105 \AA for all non-H atoms; Fig. 1). Compound (Vc) crystallized as a hemisolvate with the DMF molecule on an inversion centre (Fig. 1). In (Vc) a dihedral angle of $11.8(1)^\circ$ is formed between the planes through the non-H atoms of 5-FC and those of 6-aminoisocytosine, while the DMF molecule, unlike in (Vb), deviates from the plane of 6-aminoisocytosine by 0.203 (4) \AA .

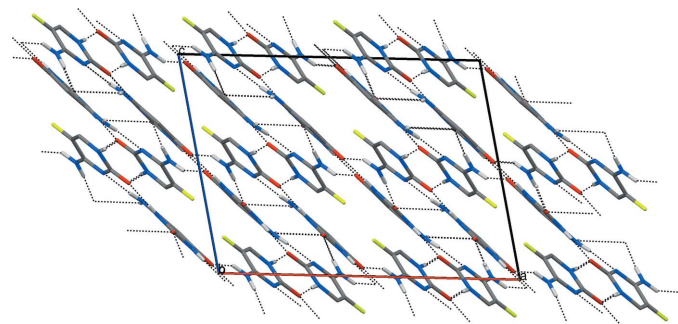


Figure 7

Packing diagram for (IV) viewed along the *b* axis, showing the three-dimensional hydrogen-bonded network. Dashed lines indicate hydrogen bonds. Only the H atoms involved in hydrogen bonding are shown.

Table 9
Hydrogen-bond geometry (Å, °) for (Va).

<i>D</i> —H··· <i>A</i>	<i>D</i> —H (Å)	H··· <i>A</i> (Å)	<i>D</i> ··· <i>A</i> (Å)	<i>D</i> —H··· <i>A</i> (°)
N3—H3···N3'	0.87 (2)	2.05 (3)	2.917 (2)	176 (2)
N61—H61 <i>B</i> ···O21' ⁱ	0.86 (3)	2.51 (3)	3.205 (2)	139 (2)
N21—H21 <i>A</i> ···O21' ⁱⁱⁱ	0.90 (2)	2.05 (2)	2.864 (2)	150 (2)
N21—H21 <i>B</i> ···O21'	0.83 (2)	2.06 (2)	2.887 (2)	174.9 (19)
N1'—H1'···O1 <i>W</i> ⁱⁱ	0.87 (3)	1.99 (3)	2.867 (2)	177 (2)
N41'—H41 <i>C</i> ···O41	0.90 (3)	2.01 (3)	2.906 (2)	171 (2)
N41'—H41 <i>D</i> ···O41 ⁱⁱⁱ	0.92 (3)	2.04 (3)	2.8441 (19)	145 (2)
O1 <i>W</i> —H1 <i>W</i> <i>A</i> ···O41 ^{iv}	0.87 (3)	1.95 (3)	2.809 (2)	170 (2)
O1 <i>W</i> —H1 <i>W</i> <i>B</i> ···N1	0.89 (3)	1.97 (3)	2.8661 (19)	175 (2)

Symmetry codes: (i) $x, y + 1, z - 1$; (ii) $-x + 1, -y, -z + 1$; (iii) $-x + 2, -y + 1, -z + 1$; (iv) $x - 1, y, z$.

Both crystal packings show layers which are parallel to (112) in (Vb) and to ($\bar{1}22$) in (Vc). Nevertheless, the molecular arrangements within the layers are different. In (Vb) the heterodimers are hydrogen-bonded to form tetramers, which are further linked to ribbons by $R_2^2(8)$ interactions involving two N—H···O hydrogen bonds between 5-FC molecules (Fig.

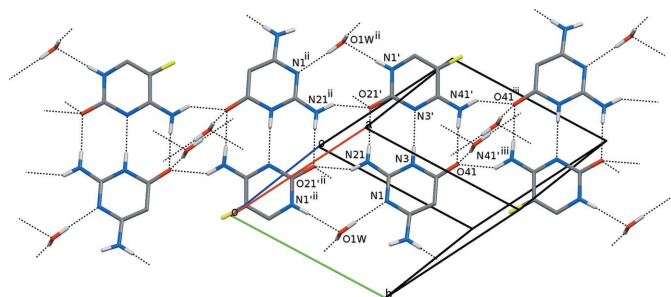


Figure 8
Partial packing diagram for (Va). Dashed lines indicate hydrogen bonds. Only the H atoms involved in hydrogen bonding are shown. Symmetry codes: (ii) $-x + 1, -y, -z + 1$; (iii) $-x + 2, -y + 1, -z + 1$.

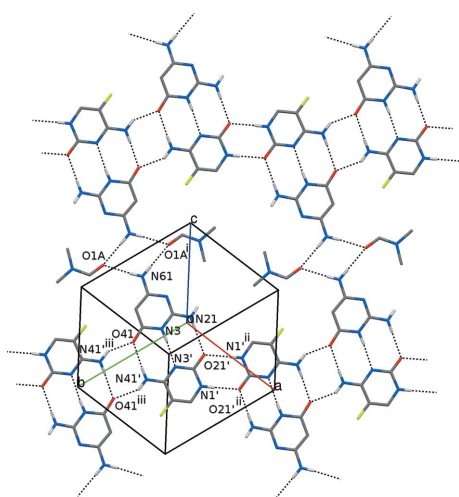


Figure 9
Partial packing diagram for (Vb). Dashed lines indicate hydrogen bonds. Only the H atoms involved in hydrogen bonding are shown. Symmetry codes: (i) $-x, -y + 1, -z + 2$; (ii) $-x + 2, -y + 1, -z + 1$; (iii) $-x + 1, -y + 2, -z + 1$.

Table 10
Hydrogen-bond geometry (Å, °) for (Vb).

<i>D</i> —H··· <i>A</i>	<i>D</i> —H (Å)	H··· <i>A</i> (Å)	<i>D</i> ··· <i>A</i> (Å)	<i>D</i> —H··· <i>A</i> (°)
N3—H3···N3'	0.889 (17)	2.063 (18)	2.941 (3)	170 (3)
N61—H61 <i>A</i> ···O1 <i>A</i>	0.886 (18)	2.077 (19)	2.958 (3)	173 (3)
N61—H61 <i>B</i> ···O1 <i>A</i> ⁱ	0.887 (18)	2.12 (2)	2.988 (3)	167 (3)
N21—H21 <i>A</i> ···O21' ⁱ	0.890 (18)	2.007 (18)	2.898 (3)	179 (3)
N1'—H1'···O21' ⁱⁱⁱ	0.879 (17)	1.872 (18)	2.748 (3)	174 (3)
N41'—H41 <i>B</i> ···O41	0.889 (17)	2.016 (18)	2.904 (3)	177 (3)
N41'—H41 <i>A</i> ···O41 ⁱⁱⁱ	0.892 (17)	1.97 (2)	2.772 (3)	148 (3)

Symmetry codes: (i) $-x, -y + 1, -z + 2$; (ii) $-x + 2, -y + 1, -z + 1$; (iii) $-x + 1, -y + 2, -z + 1$.

9, Table 10). Two DMF molecules are $R_4^2(8)$ N—H···O hydrogen-bonded to two 6-aminoisocytosine molecules thus connecting the ribbons to layers. In contrast to (Vb) the layers of (Vc) reveal hydrogen-bonded circular assemblies, each consisting of four tetramers and a disordered DMF molecule located in the centre (Fig. 10). The tetramers are connected either by two N—H···O interactions between 5-FC molecules or by two N—H···N hydrogen bonds between 6-aminoisocytosine molecules (Table 11). Altogether the crystal packing shows a three-dimensional hydrogen-bonded network.

The asymmetric unit of the third DMF solvate, (Vd), consists of three symmetry-independent complexes, each containing two 5-FC molecules, one 6-aminoisocytosine and one DMF molecule (Fig. 1). While an AAD/DDA heterodimer is formed between 6-aminoisocytosine and 5-FC, two 5-FC molecules are held together by one N—H···O and one N—H···N hydrogen bond with an $R_2^2(8)$ pattern. The 6-aminoisocytosine and the DMF molecule are essentially coplanar (r.m.s. deviations = 0.107, 0.087 and 0.054 Å for the first, the second and the third complex) and are linked by one N—H···O hydrogen bond. The DMF molecule *X* is disordered

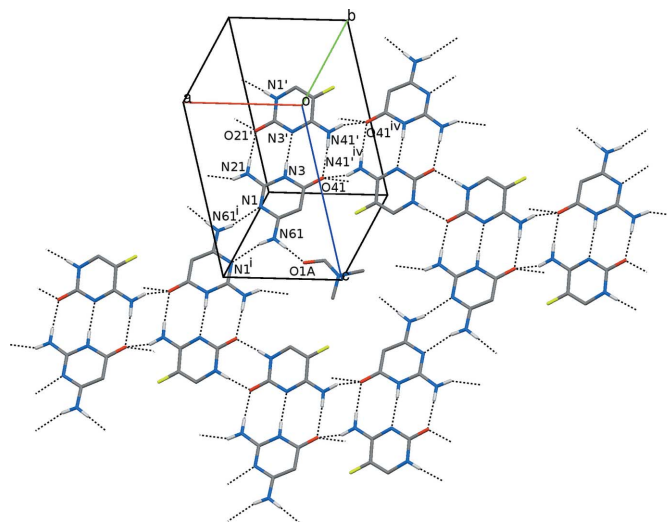


Figure 10
Partial packing diagram for (Vc). Dashed lines indicate hydrogen bonds. Only one site of the disordered solvent molecule and the H atoms involved in hydrogen bonding are shown. Symmetry codes: (i) $-x + 2, -y + 1, -z + 2$; (iv) $-x, -y + 1, -z + 1$.

Table 11
Hydrogen-bond geometry (Å, °) for (Vc).

<i>D</i> —H··· <i>A</i>	<i>D</i> —H (Å)	H··· <i>A</i> (Å)	<i>D</i> ··· <i>A</i> (Å)	<i>D</i> —H··· <i>A</i> (°)
N3—H3···N3'	0.91 (4)	2.00 (4)	2.907 (3)	178 (3)
N61—H61 <i>B</i> ···N1 ⁱ	0.883 (19)	2.16 (2)	3.031 (4)	169 (4)
N61—H61 <i>A</i> ···O1 <i>A</i>	0.902 (19)	2.17 (3)	2.931 (8)	141 (3)
N21—H21 <i>B</i> ···O41 ⁱⁱⁱ	0.85 (4)	2.31 (4)	3.080 (3)	150 (3)
N21—H21 <i>A</i> ···O21'	0.90 (4)	2.03 (4)	2.932 (3)	175 (3)
N1'—H1'···O21 ⁱⁱⁱ	0.89 (2)	1.85 (2)	2.742 (3)	179 (5)
N41'—H41 <i>B</i> ···O41	0.91 (4)	1.96 (4)	2.863 (3)	172 (3)
N41'—H41 <i>A</i> ···O41 ^{iv}	0.90 (4)	2.05 (4)	2.885 (4)	153 (3)

Symmetry codes: (i) $-x+2, -y+1, -z+2$; (ii) $x+1, y, z$; (iii) $-x+2, -y+2, -z+1$; (iv) $-x, -y+1, -z+1$.

over two sites with all non-H atoms of these sites in a common plane (r.m.s. deviation = 0.040 Å).

The crystal packing of (Vd) shows two kinds of layers parallel to (101) with similar hydrogen-bonding arrangements but with different contents: in one layer the first complex is connected only to its symmetry equivalents (Fig. 11*a*), whereas the other layer consists of symmetry equivalents of the second and the third complex (Fig. 11*b*). The following hydrogen-bonding patterns are observed within the layers (Table 12): an $R_2^2(8)$ pattern with two N—H···O bonds between 5-FC molecules, an $R_2^2(8)$ pattern with two N—H···N bonds between 6-aminoisocytosine molecules, an $R_4^2(8)$ pattern with four N—H···O bonds between two heterodimers and an $R_5^3(12)$ pattern with one N—H···N hydrogen bond and four N—H···O hydrogen bonds between two molecules of 5-FC and 6-aminoisocytosine, respectively, as well as one solvent molecule (Fig. 12). Considering only these hydrogen-bond patterns it seems that the second and the third complex are related by a pseudo-inversion centre. However, the geometrical arrangements of the main cocrystal components of the

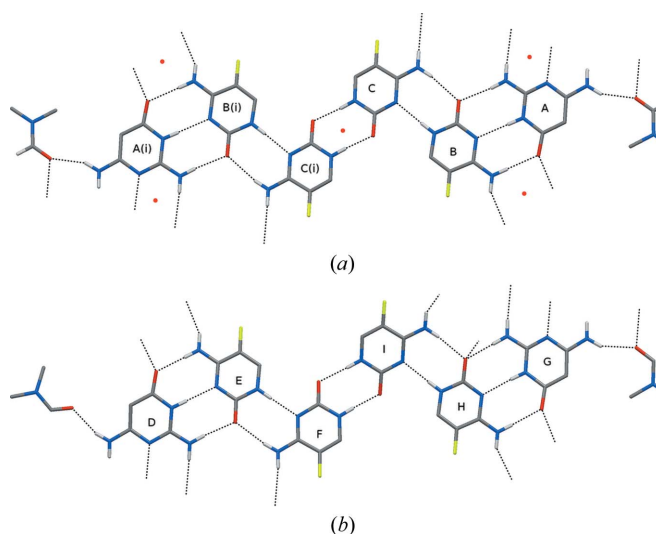


Figure 11
Hydrogen-bonding interactions in (Vd): (a) between the first complex and its symmetry equivalent; (b) between the second and the third complex. Dashed lines indicate hydrogen bonds and red dots inversion centres. Only the major occupied sites of the disordered solvent molecules and the H atoms involved in hydrogen bonding are shown.

Table 12
Hydrogen-bond geometry (Å, °) for (Vd).

<i>D</i> —H··· <i>A</i>	<i>D</i> —H (Å)	H··· <i>A</i> (Å)	<i>D</i> ··· <i>A</i> (Å)	<i>D</i> —H··· <i>A</i> (°)
N3 <i>A</i> —H3 <i>A</i> ···N3 <i>B</i>	0.87 (4)	2.02 (5)	2.894 (5)	178 (4)
N21 <i>A</i> —H21 <i>A</i> ···N1 <i>A</i> ⁱ	0.865 (19)	2.11 (2)	2.977 (4)	178 (4)
N21 <i>A</i> —H21 <i>B</i> ···O21 <i>B</i>	0.880 (19)	2.03 (2)	2.909 (5)	178 (4)
N61 <i>A</i> —H61 <i>B</i> ···O1 <i>X</i>	0.890 (19)	2.02 (2)	2.884 (5)	164 (4)
N1 <i>B</i> —H1 <i>B</i> ···N3 <i>C</i>	0.873 (19)	1.94 (2)	2.815 (4)	177 (4)
N41 <i>B</i> —H41 <i>A</i> ···O41 <i>A</i>	0.892 (19)	1.99 (2)	2.878 (5)	174 (4)
N41 <i>B</i> —H41 <i>B</i> ···O41 <i>A</i> ⁱⁱ	0.862 (19)	2.05 (3)	2.860 (4)	156 (4)
N1 <i>C</i> —H1 <i>C</i> ···O21 <i>C</i> ⁱⁱⁱ	0.86 (5)	1.92 (5)	2.780 (5)	178 (4)
N41 <i>C</i> —H41 <i>D</i> ···O21 <i>B</i>	0.893 (19)	2.13 (2)	3.010 (4)	167 (4)
N41 <i>C</i> —H41 <i>C</i> ···O1 <i>X</i> ⁱ	0.883 (19)	2.25 (2)	3.094 (4)	160 (4)
N3 <i>D</i> —H3 <i>D</i> ···N3 <i>E</i>	0.903 (19)	2.00 (2)	2.898 (5)	177 (4)
N21 <i>D</i> —H21 <i>D</i> ···N1 <i>G</i> ^{iv}	0.88 (4)	2.13 (4)	2.996 (4)	173 (4)
N21 <i>D</i> —H21 <i>C</i> ···O21 <i>E</i>	0.87 (5)	2.05 (5)	2.903 (5)	167 (4)
N61 <i>D</i> —H61 <i>D</i> ···O1 <i>Y</i>	0.902 (19)	2.01 (2)	2.885 (4)	163 (4)
N1 <i>E</i> —H1 <i>E</i> ···N3 <i>F</i>	0.882 (19)	1.93 (2)	2.801 (4)	172 (4)
N41 <i>E</i> —H41 <i>F</i> ···O41 <i>D</i>	0.893 (19)	1.97 (2)	2.861 (5)	175 (4)
N41 <i>E</i> —H41 <i>E</i> ···O41 <i>G</i> ^v	0.889 (19)	2.08 (3)	2.895 (4)	151 (4)
N1 <i>F</i> —H1 <i>F</i> ···O21 <i>I</i>	0.889 (19)	1.89 (2)	2.768 (4)	168 (4)
N41 <i>F</i> —H41 <i>H</i> ···O21 <i>E</i>	0.877 (19)	2.12 (2)	2.999 (4)	179 (4)
N41 <i>F</i> —H41 <i>G</i> ···O1 <i>Z</i> ^{iv}	0.882 (19)	2.23 (2)	3.112 (4)	173 (4)
N3 <i>G</i> —H3 <i>G</i> ···N3 <i>H</i>	0.876 (19)	2.03 (2)	2.904 (5)	174 (4)
N21 <i>G</i> —H21 <i>F</i> ···N1 <i>D</i> ^{vi}	0.88 (4)	2.09 (4)	2.968 (4)	176 (4)
N21 <i>G</i> —H21 <i>E</i> ···O21 <i>H</i>	0.91 (5)	2.03 (5)	2.933 (5)	171 (3)
N61 <i>G</i> —H61 <i>F</i> ···O1 <i>Z</i>	0.89 (5)	2.05 (5)	2.866 (5)	153 (4)
N1 <i>H</i> —H1 <i>H</i> ···N3 <i>I</i>	0.870 (19)	1.94 (2)	2.809 (4)	176 (4)
N41 <i>H</i> —H41 <i>I</i> ···O41 <i>G</i>	0.896 (19)	1.97 (2)	2.865 (5)	173 (4)
N41 <i>H</i> —H41 <i>J</i> ···O41 <i>D</i> ^{vii}	0.885 (19)	2.09 (3)	2.847 (4)	143 (4)
N1 <i>I</i> —H1 <i>I</i> ···O21 <i>F</i>	0.868 (19)	1.90 (2)	2.762 (4)	173 (4)
N41 <i>I</i> —H41 <i>L</i> ···O21 <i>H</i>	0.904 (19)	2.07 (2)	2.974 (4)	174 (4)
N41 <i>I</i> —H41 <i>K</i> ···O21 <i>H</i> ^{viii}	0.880 (18)	2.31 (3)	3.068 (4)	144 (3)

Symmetry codes: (i) $-x, -y+1, -z+1$; (ii) $-x, -y+2, -z+1$; (iii) $-x+1, -y+2, -z$; (iv) $x+1, y+1, z-1$; (v) $x+1, y, z-1$; (vi) $x-1, y-1, z+1$; (vii) $x-1, y, z+1$; (viii) $-x, -y, -z+2$.

latter two complexes are different. In the second complex, a dihedral angle of 8.8 (1)° is formed between the planes through the non-H atoms of the heterodimer components, while the two 5-FC molecules are coplanar (r.m.s. deviation = 0.047 Å for all non-H atoms). In the third complex the planes through the non-H atoms of the heterodimer components enclose a similar dihedral angle of 7.2 (1)°, but the dihedral

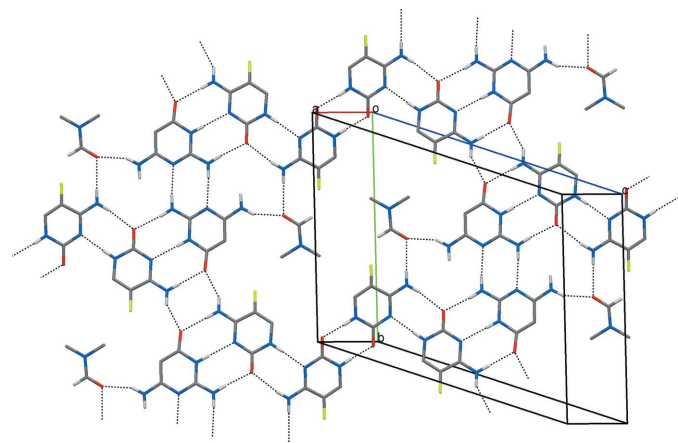


Figure 12
Partial packing diagram for (Vd). Dashed lines indicate hydrogen bonds. Only the H atoms involved in hydrogen bonding are shown.

angle of $9.6(1)^\circ$ between the planes through their non-H atoms reveals that the two 5-FC molecules are not coplanar. The crystal packing is dominated by these layers; in addition, $N-H \cdots O$ hydrogen bonds link adjacent layers.

3.3. Cocrystal with acyclovir

As mentioned in §1 the combination of 5-FC and the bacterial CD gene is used for the treatment of cancer (Huber *et al.*, 1994). However, high doses of 5-FC are necessary, which may lead to undesirable side effects (Kievit *et al.*, 1999). A potential method to overcome this limitation is the double-suicide gene therapy (Aghi *et al.*, 1998; Boucher *et al.*, 2006). The combination of 5-FC and the bacterial CD gene with the guanine derivative ganciclovir and the enzyme herpes simplex virus thymidine kinase has been proven to enhance the anticancer effect in comparison with the monotherapies. Ganciclovir is also a prodrug used for the treatment of cytomegalovirus infections; ganciclovir triphosphate is incorporated into DNA instead of guanosine triphosphate and, as a result, inhibits the cellular DNA polymerase (Littler *et al.*, 1992; Sullivan *et al.*, 1992).

Almost all studies investigated the combination of 5-FC with ganciclovir, although a comparable synergism is observed between 5-FC and acyclovir (Aghi *et al.*, 1998). Acyclovir differs from ganciclovir by the absence of a hydroxymethyl group at the 3' position of the acyclic side chain. It is a prodrug for the treatment of herpes-simplex, varicella-zoster as well as Epstein-Barr virus infections (Balfour, 1999). However, the routes of administration of both drugs are different: ganciclovir is administered intravenously, but acyclovir orally. Also for this reason the combination of 5-FC and acyclovir might be interesting.

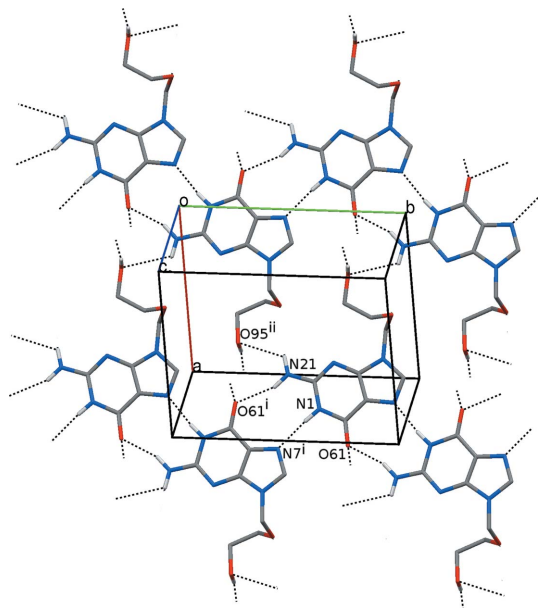


Figure 13
Partial packing diagram for (VI). Dashed lines indicate hydrogen bonds. Only the H atoms involved in hydrogen bonding are shown. Symmetry codes: (i) $-x + 2, y - \frac{1}{2}, -z + \frac{3}{2}$; (ii) $-x + 1, y - \frac{1}{2}, -z + \frac{1}{2}$.

Table 13
Selected torsion angles ($^\circ$) of acyclovir in (VI) and (VII).

Torsion angle ($^\circ$)	(VI)	(VII)
C8–N9–C91–O92	–74.3 (3)	73.11 (16)
N9–C91–O92–C93	–58.4 (3)	77.46 (15)
C91–O92–C93–C94	–71.4 (3)	–171.75 (13)
O92–C93–C94–O95	–59.1 (3)	–63.25 (18)

Since the first medical use of acyclovir in 1983, only the crystal structure of a hydrate [refcodes CEHTAK (Birnbbaum *et al.*, 1981) and CEHTAK10 (Birnbbaum *et al.*, 1984)], but no solvent-free structure, has been published. In addition to the desired cocrystal of 5-FC and acyclovir, (VII), a solvent-free structure of acyclovir, (VI), was obtained during our crystallization experiments (Fig. 1).

In (VI) the glycosidic torsion angle C8–N9–C91–O92 to the planar guanine residue (r.m.s. deviation for all non-H atoms = 0.013 \AA) is $-74.3(3)^\circ$, and the side chain C–O and C–C bonds are also in the synclinal conformation (Table 13). In the crystal packing the acyclovir molecules are connected to chains running along the *b* axis by one $N-H \cdots O$ and one $N-H \cdots N$ hydrogen bond with an $R_2^2(9)$ motif (Fig. 13, Table 14). Further $N-H \cdots O$ hydrogen bonds connect adjacent chains to layers parallel to $(\bar{3}02)$. Stacking interactions along the *c* axis and $O-H \cdots O$ hydrogen bonds also contribute to the structural stability (Fig. 14).

In the cocrystal of 5-FC with acyclovir (VII) both molecules are linked by three hydrogen bonds with a pattern similar to the Watson–Crick C–G base pair, whereby the pyrimidine and purine rings are coplanar to each other (r.m.s. deviation = 0.040 \AA for all non-H atoms; Fig. 1). The glycosidic torsion angle of acyclovir as well as the conformation about the C91–O92 and C93–C94 bonds are in agreement with (VI), but the C91 and C94 atoms are now in an antiperiplanar arrangement (Table 13). In the crystal packing the heterodimers of 5-FC and acyclovir are further connected to each other through inversion centres by two $N-H \cdots N$ hydrogen bonds. Stacking interactions help to stabilize the crystal structure (Fig. 15). Along the *b* axis the heterodimers are connected by bifurcated hydrogen bonds from the O–H group (Fig. 16, Table 15). Furthermore, $N-H \cdots O$ hydrogen bonds link the heterodimers to zigzag chains running along the *c* axis, so that

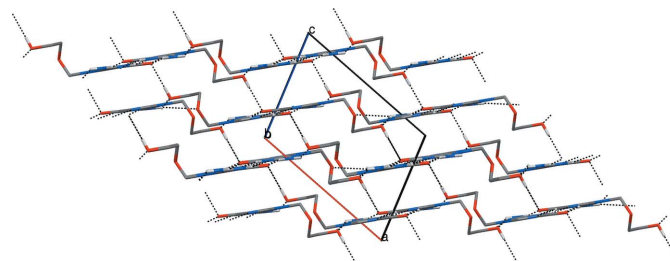


Figure 14
Packing diagram for (VI) viewed along the *b* axis, showing the three-dimensional hydrogen-bonded network. Dashed lines indicate hydrogen bonds. Only the H atoms involved in hydrogen bonding are shown.

Table 14
Hydrogen-bond geometry (Å, °) for (VI).

$D-H\cdots A$	$D-H$ (Å)	$H\cdots A$ (Å)	$D\cdots A$ (Å)	$D-H\cdots A$ (°)
$N1-H1\cdots N7^i$	0.885 (18)	1.960 (19)	2.834 (3)	169 (3)
$N21-H21A\cdots O95^{ii}$	0.864 (19)	2.56 (3)	3.069 (3)	118 (3)
$N21-H21B\cdots O61^i$	0.881 (19)	2.09 (2)	2.934 (3)	159 (3)
$O95-H95\cdots O61^{iii}$	0.84	2.01	2.849 (3)	174.8

Symmetry codes: (i) $-x+2, y-\frac{1}{2}, -z+\frac{3}{2}$; (ii) $-x+1, y-\frac{1}{2}, -z+\frac{1}{2}$; (iii) $x-1, -y+\frac{3}{2}, z-\frac{1}{2}$.

altogether a three-dimensional hydrogen-bonded network is formed.

4. Discussion

Since the formation of hydrogen bonds in crystal structures is affected by many factors, cocrystal synthesis is not a straightforward process. In spite of the complementary binding sites, the expected hydrogen-bonding pattern is not observed in (III) and (IV). In (I) 5-FC and 2-aminopyrimidine are connected to the desired $R_2^2(8)$ heterodimer, but one may ask if perhaps other $R_2^2(8)$ hydrogen-bonded arrangements between these components are comparably stabilized. In most structures containing 5-FC, the formation of its homodimers is preferred. Although all dimers of 5-FC show an $R_2^2(8)$ pattern, they consist of different types of hydrogen bonds. Since they appear in different frequency, we have tried to investigate their relative stabilities.

Hence *ab initio* energy calculations were carried out for selected complexes and their respective components. The difference between the energy of a complex and the sum of the energies of its components gives an estimate of the energy of complex formation (Table 16).

The $R_2^2(8)$ homodimers of 5-FC are stabilized by one $N-H\cdots O$ and one $N-H\cdots N$ hydrogen bond (*dim1*) in almost all (pseudo)polymorphs; only in one monohydrate structure of 5-FC, homodimers with two $N-H\cdots O$ (*dim2*) or two $N-H\cdots N$ hydrogen bonds (*dim3*) are observed. The result of the *ab initio* energy calculations confirms the relative stabilities of

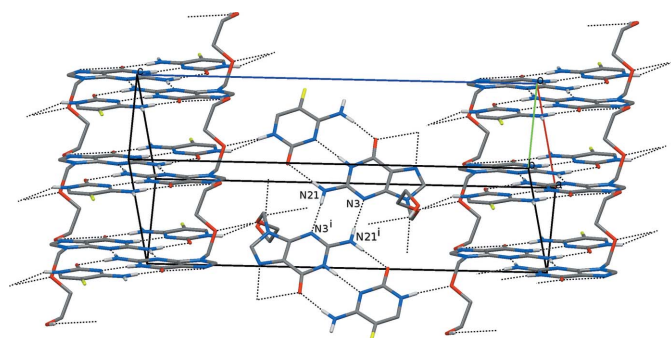


Figure 15
Partial packing diagram for (VII). Dashed lines indicate hydrogen bonds. Only the H atoms involved in hydrogen bonding are shown. Symmetry code: (i) $-x+1, -y+2, -z+1$.

Table 15
Hydrogen-bond geometry (Å, °) for (VII).

$D-H\cdots A$	$D-H$ (Å)	$H\cdots A$ (Å)	$D\cdots A$ (Å)	$D-H\cdots A$ (°)
$N1-H1\cdots N3'$	0.895 (15)	2.002 (15)	2.8964 (18)	176.3 (17)
$N21-H21B\cdots N3^i$	0.87 (2)	2.20 (2)	3.0698 (19)	177 (2)
$N21-H21A\cdots O21'$	0.88 (2)	2.05 (2)	2.9317 (19)	179.7 (19)
$O95-H95\cdots N7^{ii}$	0.84	2.32	3.0663 (18)	147.7
$O95-H95\cdots O61^{ii}$	0.84	2.47	3.1112 (16)	133.5
$N1'-H1'\cdots O92^{iii}$	0.88 (2)	2.22 (2)	3.0246 (18)	151.6 (19)
$N41'-H41A\cdots O61$	0.908 (16)	1.878 (16)	2.7844 (18)	175 (2)

Symmetry codes: (i) $-x+1, -y+2, -z+1$; (ii) $x, y+1, z$; (iii) $x, -y+\frac{3}{2}, z+\frac{1}{2}$.

these homodimers: *dim1* is energetically most favourable; the energy of *dim2* differs only slightly from that of *dim1* ($\Delta E = 0.5 \text{ kJ mol}^{-1}$), while *dim3* seems to be less stable.

The 5-FC and 2-aminopyrimidine molecules can be connected either by one $N-H\cdots O$ and one $N-H\cdots N$ hydrogen bond (*dim4*) or by two $N-H\cdots N$ bonds (*dim5*). In (I) the energetically more favourable heterodimer *dim4* is formed. However, the energy difference between *dim4* and *dim5* of 3.0 kJ mol^{-1} is rather small, so the formation of *dim5* in other polymorphic structures seems possible. In addition to the heterodimers, $R_2^2(8)$ homodimers of 5-FC are observed in this cocrystal. Here the energetically less favourable homodimer *dim3* is formed since the $C=O$ and $N-H$ groups of the 5-FC molecule, which are required for the formation of the more favourable homodimers *dim1* and *dim2*, participate already in the interaction with the 2-aminopyrimidine molecule.

The heterodimers between 5-FC and *N*-acetylcreatine can be stabilized either by one $N-H\cdots O$ and one $N-H\cdots N$ hydrogen bond (*dim6*) or by two $N-H\cdots O$ bonds (*dim7*). Such heterodimers are not observed in (III); the cocrystal

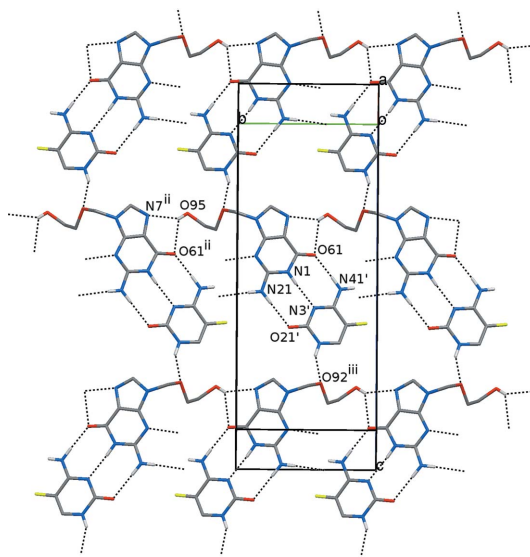
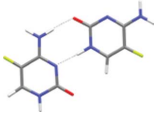
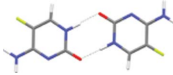
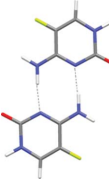
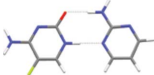
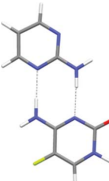
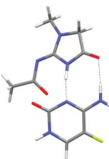
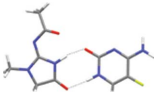
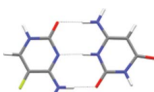
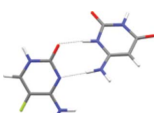
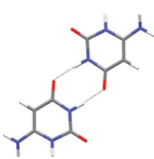


Figure 16
Partial packing diagram for (VII). Dashed lines indicate hydrogen bonds. Only the H atoms involved in hydrogen bonding are shown. Symmetry codes: (ii) $x, y+1, z$; (iii) $x, -y+\frac{3}{2}, z+\frac{1}{2}$.

Table 16
Hydrogen-bonding patterns and the energies released during complex formation.

Name	Hydrogen-bonding pattern	Energy (kJ mol ⁻¹)
<i>dim1</i>		-101.6
<i>dim2</i>		-101.1
<i>dim3</i>		-92.0
<i>dim4</i>		-71.3
<i>dim5</i>		-68.3
<i>dim6</i>		-54.7
<i>dim7</i>		-48.7
<i>dim8</i>		-122.1
<i>dim9</i>		-64.8
<i>dim10</i>		-57.8

components are connected merely by a single N—H···O hydrogen bond. Looking at the molecular arrangements in *dim6* and *dim7*, the formation of the desired heterodimer is hindered by the repulsion of the neighbouring carbonyl O atoms. In (III) $R_2^2(8)$ homodimers of 5-FC with one N—H···O and one N—H···N hydrogen bond (*dim1*) are formed. A comparison of the energies of *dim1*, *dim6* and *dim7* may

explain the hydrogen-bonding interactions observed in (III). The energy released during the formation of *dim6* or *dim7* would be 54.7 or 48.7 kJ mol⁻¹, while the formation of *dim1* leads to an energy release of 101.6 kJ mol⁻¹. Therefore, the 5-FC molecules prefer the formation of homodimers instead of heterodimers.

Due to their complementary *AAD/DDA* binding sites, the 5-FC and 6-aminouracil molecules should be able to form a heterodimer with three hydrogen bonds and a calculated energy release of 122.1 kJ mol⁻¹ (*dim8*). In cocrystal (IV), however, both molecules are only connected by one N—H···O and one N—H···N hydrogen bond (*dim9*) with a much higher energy of -64.8 kJ mol⁻¹. In (IV) and in *dim9* though, the 5-FC and 6-aminouracil molecules show a significantly different arrangement: in (IV) the dihedral angle between the two molecules is 19.7 (1)°, while in *dim9* the calculated dihedral angle is approximately 45° probably because of the repulsion of the amino groups. In addition to *dim9*, $R_2^2(8)$ homodimers of 5-FC (*dim2*) and of 6-aminouracil (*dim10*) each characterized by two N—H···O hydrogen bonds are observed in (IV). Similar interactions are also found in the monohydrate structure of 5-FC [refcode BIRMEU03 (Hulme & Tocher, 2006)] and in the solvent-free structure of 6-aminouracil [refcode COTVIR (Golovina *et al.*, 2008)]. The energy released during the formation of *dim2* and *dim10* (101.1 kJ mol⁻¹ for *dim2* and 57.8 kJ mol⁻¹ for *dim10*) might be sufficient to compensate the energy difference of 57.3 kJ mol⁻¹ between *dim8* and *dim9*. It is noteworthy that the interplay of the hydrogen-bonding interactions in *dim2*, *dim9* and *dim10* leads to a calculated density of 1.650 g cm⁻³ in (IV), which is relatively high for organic crystals.

In addition to the desired *AAD/DDA* heterodimers, $R_2^2(8)$ homodimers of the cocrystal components are observed in the cocrystals of 5-FC and 6-aminoisocytosine. In (Vb) and (Vc) the $R_2^2(8)$ homodimers of 5-FC are characterized by two N—H···O hydrogen bonds, while in (Vd) they are stabilized either by one N—H···O and one N—H···N hydrogen bond or by two N—H···O hydrogen bonds. $R_2^2(8)$ homodimers of 6-aminoisocytosine with two N—H···N hydrogen bonds are formed in (Vc) and (Vd). The cocrystal of 5-FC with acyclovir (VII) confirms the stability of the *AAD/DDA* hydrogen-bonding pattern. Homodimers of acyclovir stabilized by two N—H···N hydrogen bonds are also observed in this crystal structure; in contrast, homodimers of 5-FC are not present.

5. Conclusions

The 5-FC and 2-aminopyrimidine molecules are connected to the desired *AD/DA* heterodimer by one N—H···O and one N—H···N hydrogen bond in (I). However, due to the relatively small energy difference the formation of a heterodimer with two N—H···N hydrogen bonds in other polymorphic structures seems possible. A similar $R_2^2(8)$ heterodimer was expected between 5-FC and *N*-acetylcreatinine, but in their cocrystal (III) both molecules are merely connected by a single hydrogen bond. In addition, the typical homodimers of 5-FC with one N—H···O and one N—H···N hydrogen bond

are observed. The quantum-mechanical calculations give a plausible explanation why homodimer formation is preferred in cocrystal (III). Despite the complementary *AAD/DDA* hydrogen-bonding sites, the heterodimer between 5-FC and 6-aminouracil is held together by only two instead of three hydrogen bonds in cocrystal (IV); in addition, homodimers with two N–H···O hydrogen bonds are formed for each component. The energy released during homodimer formation is likely to be sufficient to compensate the energy difference to the *AAD/DDA* heterodimer. Finally, the four cocrystals of 5-FC and 6-aminoisocytosine, (Va)–(Vd), and the cocrystal with the antiviral drug acyclovir, (VII), confirm the stability of the *AAD/DDA* hydrogen-bonding pattern.

All cofomers studied hitherto reveal fixed hydrogen-bonding sites complementary to those of 5-FC. We have also investigated the influence of complex formation on the conformational or the tautomeric equilibrium of compounds. The results will be presented in the sequel of this paper (Tutughamiarso & Egert, 2012).

We thank Karol Hinz for the crystallization of compound (II) and Dr Michael Bolte for helpful discussions.

References

- Aghi, M., Kramm, C. M., Chou, T. C., Breakefield, X. O. & Chiocca, E. A. (1998). *J. Natl Cancer Inst.* **90**, 370–380.
- Allen, F. H. (2002). *Acta Cryst.* **B58**, 380–388.
- Balfour, H. H. (1999). *N. Engl. J. Med.* **340**, 1255–1268.
- Benson, J. M. & Nahata, M. C. (1988). *Clin. Pharm.* **7**, 424–438.
- Bernstein, J., Davis, R. E., Shimon, L. & Chang, N.-L. (1995). *Angew. Chem. Int. Ed. Engl.* **34**, 1555–1573.
- Birnbaum, G. I., Cygler, M., Kusmier, J. T. & Shugar, D. (1981). *Biochem. Biophys. Res. Commun.* **103**, 968–974.
- Birnbaum, G. I., Cygler, M. & Shugar, D. (1984). *Can. J. Chem.* **62**, 2646–2652.
- Boucher, P. D., Im, M. M., Freytag, S. O. & Shewach, D. S. (2006). *Cancer Res.* **66**, 3230–3237.
- Desiraju, G. R. (1995). *Angew. Chem. Int. Ed. Engl.* **34**, 2311–2327.
- Francis, P. & Walsh, T. J. (1992). *Clin. Infect. Dis.* **15**, 1003–1018.
- Frisch, M. J. *et al.* (2004). *GAUSSIAN03*. Gaussian Inc., Wallingford, CT, USA.
- Golovina, N. I., Nechiporenko, G. N., Zyuzin, I. N., Lempert, D. B., Nemtsev, G. G., Shilov, G. V., Utenyshev, A. N. & Bozhenko, K. V. (2008). *J. Struct. Chem.* **49**, 909–916.
- Huber, B. E., Austin, E. A., Richards, C. A., Davis, S. T. & Good, S. S. (1994). *Proc. Natl Acad. Sci. USA*, **91**, 8302–8306.
- Hulme, A. T. & Tocher, D. A. (2006). *Cryst. Growth Des.* **6**, 481–487.
- Kievit, E., Bershad, E., Ng, E., Sethna, P., Dev, I., Lawrence, T. S. & Rehemtulla, A. (1999). *Cancer Res.* **59**, 1417–1421.
- Littler, E., Stuart, A. D. & Chee, M. S. (1992). *Nature*, **358**, 160–162.
- Macrae, C. F., Bruno, I. J., Chisholm, J. A., Edgington, P. R., McCabe, P., Pidcock, E., Rodriguez-Monge, L., Taylor, R., van de Streek, J. & Wood, P. A. (2008). *J. Appl. Cryst.* **41**, 466–470.
- Morschhäuser, J. (2003). *Pharm. Unserer Zeit*, **32**, 124–128.
- Sheldrick, G. M. (2008). *Acta Cryst.* **A64**, 112–122.
- Stoe & Cie (2001). *X-AREA*. Stoe & Cie, Darmstadt, Germany.
- Sullivan, V., Talarico, C. L., Stanat, S. C., Davis, M., Coen, D. M. & Biron, K. K. (1992). *Nature*, **358**, 162–164.
- Tutughamiarso, M., Bolte, M. & Egert, E. (2009). *Acta Cryst.* **C65**, o574–o578.
- Tutughamiarso, M. & Egert, E. (2012). *Acta Cryst.* **B68**, 444–452.
- Vermes, A., Guchelaar, H. J. & Dankert, J. (2000). *J. Antimicrob. Chemother.* **46**, 171–179.
- Vishweshwar, P., McMahon, J. A., Bis, J. A. & Zaworotko, M. J. (2006). *J. Pharm. Sci.* **95**, 499–516.
- Yadav, A. V., Shete, A. S., Dabke, A. P., Kulkarni, P. V. & Sakhare, S. S. (2009). *Indian J. Pharm. Sci.* **71**, 359–370.
- Zerkowski, J. A. & Whitesides, G. M. (1994). *J. Am. Chem. Soc.* **116**, 4298–4304.